Accuracy and Precision of Regional Multiharmonic Fourier Analysis of Gated Blood-Pool Images

Josef Machac, Steven F. Horowitz, David Broder, and Stanley J. Goldsmith

In order to estimate the precision and accuracy of parameters derived from segmental multiharmonic Fourier analysis of gated blood-pool images, a Monte Carlo computer noise simulation was tested on five sample regional time-activity curves. The first three Fourier harmonics were retained and the precision and accuracy of parameters of ventricular function were calculated, varying the ejection fraction, segment size, and framing rate. Precision improved with higher ejection fraction, higher counts per frame, or higher framing rate. There was no change in precision as the framing rate changed at fixed total counts. Accuracy changed little with changing framing rate. Thus, for segmental analysis there is no advantage to using a higher framing rate. Regions five or more pixels in size are recommended for reliable results. This study provides useful information for the optimization of acquisition and processing conditions for regional gated blood-pool analysis.

J Nucl Med 25: 1294–1299, 1984

There has been much interest in regional gated blood-pool analysis in the form of parametric images and segmental time-activity curves. The phase and amplitude derived from the first harmonic of the Fourier transform of the regional time-activity curve have been used as an objective quantitative measure of regional wall motion (*1–6*). Multiharmonic analysis has been proposed to overcome the shortcomings of the first harmonic, which include distortion of the original data and lack of specificity of the phase for any particular part of the cardiac cycle (*7*). The original time-activity curve is more faithfully represented by including two or more harmonics of the curve's Fourier series, thus producing a continuous, interpolated, fitted curve. From this curve, several parameters specific for each of its different aspects can be calculated (*7–9*). These include the time of end-systole, time of end-diastole, times of maximum ejection rate and filling rate, maximum ejection rate and filling rate, and the ejection fraction. Interest has been generated in the analysis of global ventricular function based on these parameters by specifying different specific features of the time-activity curve (*10–12*).

Received Dec. 22, 1983; revision accepted Aug. 21, 1984.

For reprints contact: Josef Machac, MD, Nuclear Cardiology, Annenberg 8, Mt. Sinai Med. Ctr., 1 Gustave Levy Place, New York, NY 10029.

The regional time-activity curve is affected by error from random noise. The current study was undertaken to determine the effect of segment size, count density, and framing rate on the precision and accuracy of parameters derived from the time-activity curve, using a Monte Carlo computer noise simulator.

METHODS

The instrument used for this study was a microprocessor equipped with a line printer. The computation program was written in BASIC. The Monte Carlo noise generator consisted of two congruential-type pseudorandom number generators, producing a uniform distribution over the range of 0 to 1. This was transformed by a cumulative Gaussian distribution, producing a distribution such that for any externally supplied number N, the error is proportional to the square root of N, resulting in an output number governed by a probability function approximating a Poisson distribution ($p \sim 0.001$) simulating random counting error.

Five commonly encountered regional time-activity curves were described by 32 points (Fig. 1, left). Each of the curves underwent a discrete Fourier transform, and a new, continuous curve was reconstructed in the time domain using all 16 harmonics, thus producing a

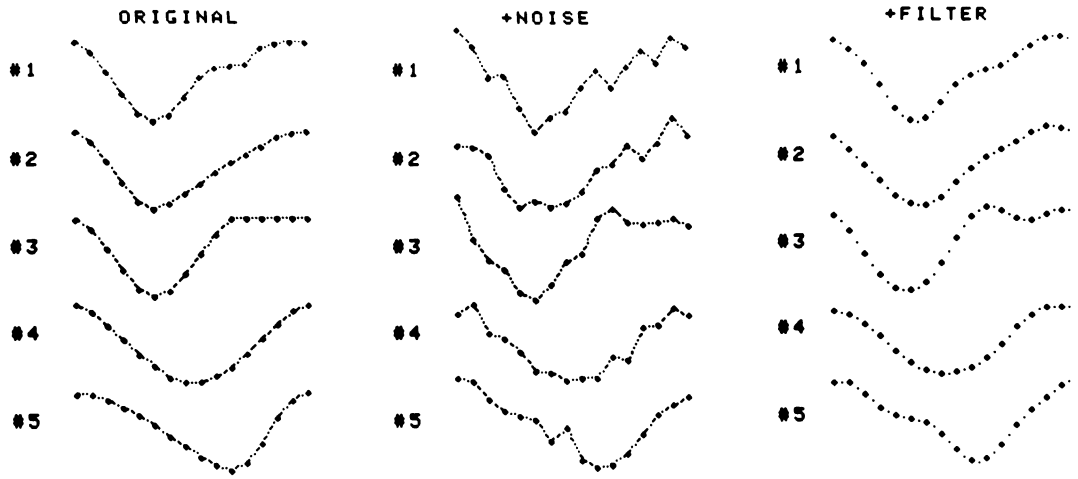

FIG. 1. Original five simulated time-activity curves (left); after superposition of Monte Carlo noise (middle); and after reconstruction in time domain of first three harmonics (right).

parametric replica of the original 32-point curve. These continuous curves were used as original templates for noise superposition, to ensure that the identical curve was sampled regardless of the framing rate. The curves were also used to calculate the noise-free parameters for the estimation of accuracy. The end-diastolic count density was set at 300 counts per pixel, a typical figure for either of the two ventricles in routine clinical images. For convenience, the temporal duration of the heart cycle was fixed at 800 msec. The curves were scaled to produce three different ejection fractions after background subtraction: 25%, 50%, and 75%, and multiplied by 1, 5, 10, 20, or 50 to simulate varying number of pixels per segment. For purposes of this model, an increase in segment size from five to ten pixels was also equivalent to a doubling of the count density per pixel while holding the segment size constant. In this manner, both an increase in segment size or counts per frame were simulated.

Each curve was sampled at 16, 24, and 32 frames per cycle under either of two conditions:

1. As the framing rate is increased, the counts per frame (counts per pixel times the region size) are held constant. The total counts in the study over all frames thus increase linearly with the framing rate. This condition would hold in routine resting radionuclide gated blood-pool studies where the time of acquisition is not critical.

2. Total counts per study over all frames are held constant and the framing rate increased. Thus, the counts per frame for any particular region size is inversely related to the framing rate. This condition would prevail during exercise studies and emergency studies where total acquisition time is limited, and one must choose between a higher framing rate or higher counts per frame.

Each of the five curves underwent 75 permutations that included three ejection fractions, five region sizes, and five framing conditions. For each of these generated curves, noise was superimposed by the Monte Carlo generator to simulate a real time-activity curve (Fig. 1, center). A Fourier transform was performed on this curve and a new curve reconstructed in the time domain using the first three harmonics only (Fig. 1, right). This is equivalent to filtering by a square-shaped, low-pass filter with a cutoff of 3 cycles per period. From this new filtered curve, the following parameters were calculated: the ejection fraction (EF), maximum ejection rate (MER), maximum filling rate (MFR), time of maximum ejection rate (TMER), time of minimum counts at end-systole (TES), time of maximum filling rate (TMFR), and the first-harmonic phase (PH_1). Except for PH_1, this was accomplished using Newton's method of iterative solution. The starting values of this iterative procedure were obtained by a cursory search of the curve. Computations were terminated when two successive computations differed in time by less than 1 msec. This resolution limit is less than the expected variation due to sampling noise. The maximum ejection rate and maximum filling rate were normalized to the counts at end-diastole. At every set of permutations of ejection fraction, region size, and framing rate, this process was repeated 100 times for a total of 37,500 trials.

The mean and standard deviation of each parameter was calculated under each set of conditions. The standard deviation was used as a measure of precision. The error of the estimate of the standard deviation of the parameters for any one curve was 8%. The collective behavior of the precision of the various calculated parameters for the five curves was plotted as a mean of the five standard deviations (± standard error of this mean) as a function of ejection fraction, segment size (counts per frame), and framing rate. Changes between values of the mean standard deviation (precision) at different conditions were tested for significance using two-tailed, two-way analysis of variance (*13*).

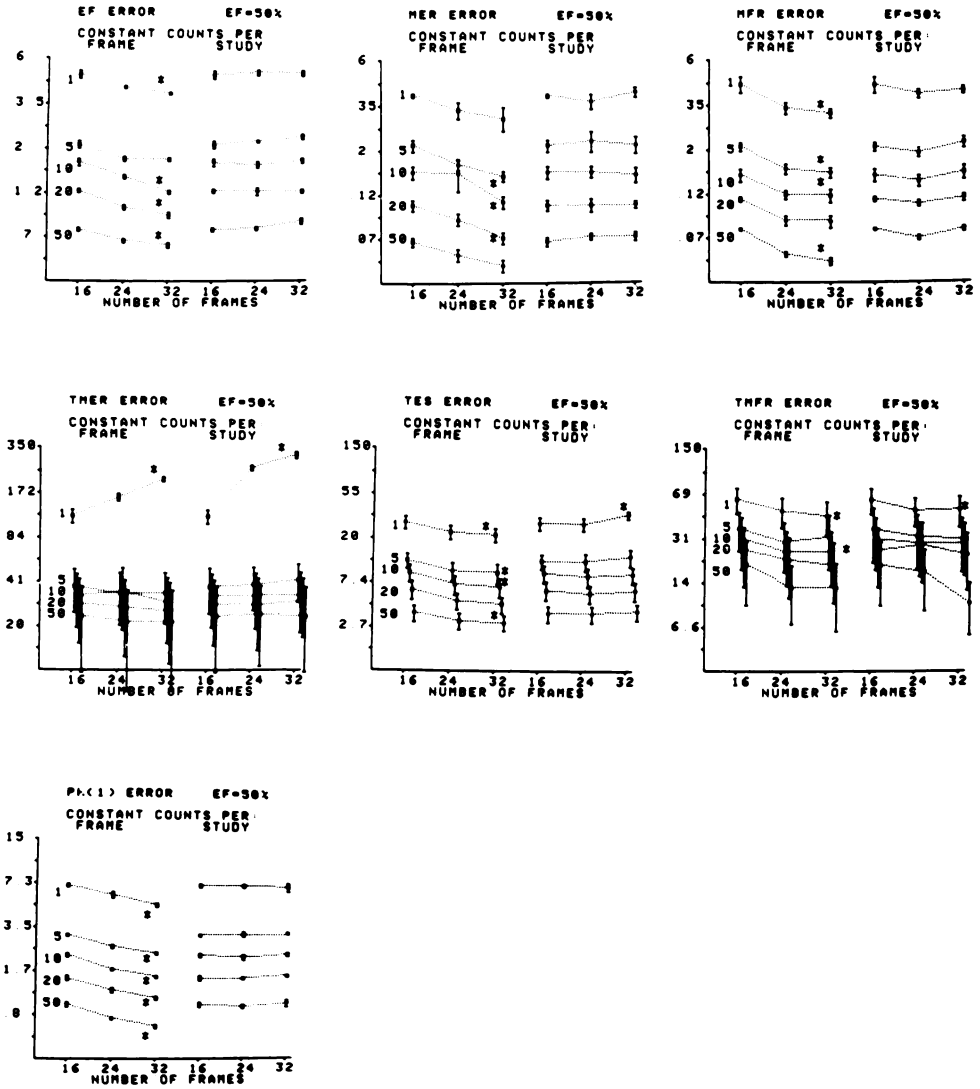

FIG. 2. Precision errors, plotted (with log ordinate) as mean standard deviations (± s.e.m.), as function of framing rate, with pixels per segment (counts per frame) as parameter. Errors are for calculated: ejection fraction (EF, %), maximum ejection rate (MER, end-diastolic volumes/sec), maximum filling rate (MFR, end-diastolic volumes/sec), time of maximum ejection rate (TMER, msec), time of end/systole (TES, msec), time of maximum filling rate (TMER, msec), and first-harmonic phase (PH_1, degrees); all at ejection fraction of 50%. * = $p < 0.05$ for differences in values at 16 and 32 frames per cycle.

For the five curves, the accuracy of the calculated parameters under each set of conditions was defined as the root-mean-square (RMS) difference between the parameter's mean values derived from the noisy curves, and the corresponding parameters derived from the original control curves. This RMS was plotted, along with bars indicating the standard error of the root mean, as a function of the various conditions, and was analyzed for changes with two-way analysis of variance.

RESULTS

The precision error of the various parameters was measured by the mean standard deviation of the five curves under a variety of conditions. With increasing ejection fraction, the absolute precision error decreases for the measured EF, TMER, TES, TMFR, and PH_1 and is unchanged for MER and MFR. (The percent relative precision error for MER and MFR, however, does decrease.) Figure 2 shows the data at an ejection fraction of 50%. The behavior of the parameter precision error at smaller and higher ejection fractions runs essentially parallel. As the segment size, and therefore the counts per frame, increases, the precision error decreases for all parameters. The precision error also decreases for the EF, MER, MFR, TES, and PH_1 as the framing rate is increased at constant counts per frame. The precision error of TMER and TMFR tends to remain the same. The same relative decrease in precision error is achieved by either increasing the framing rate while maintaining constant counts per frame, or by increasing the counts per frame, (segment size or count density) while keeping

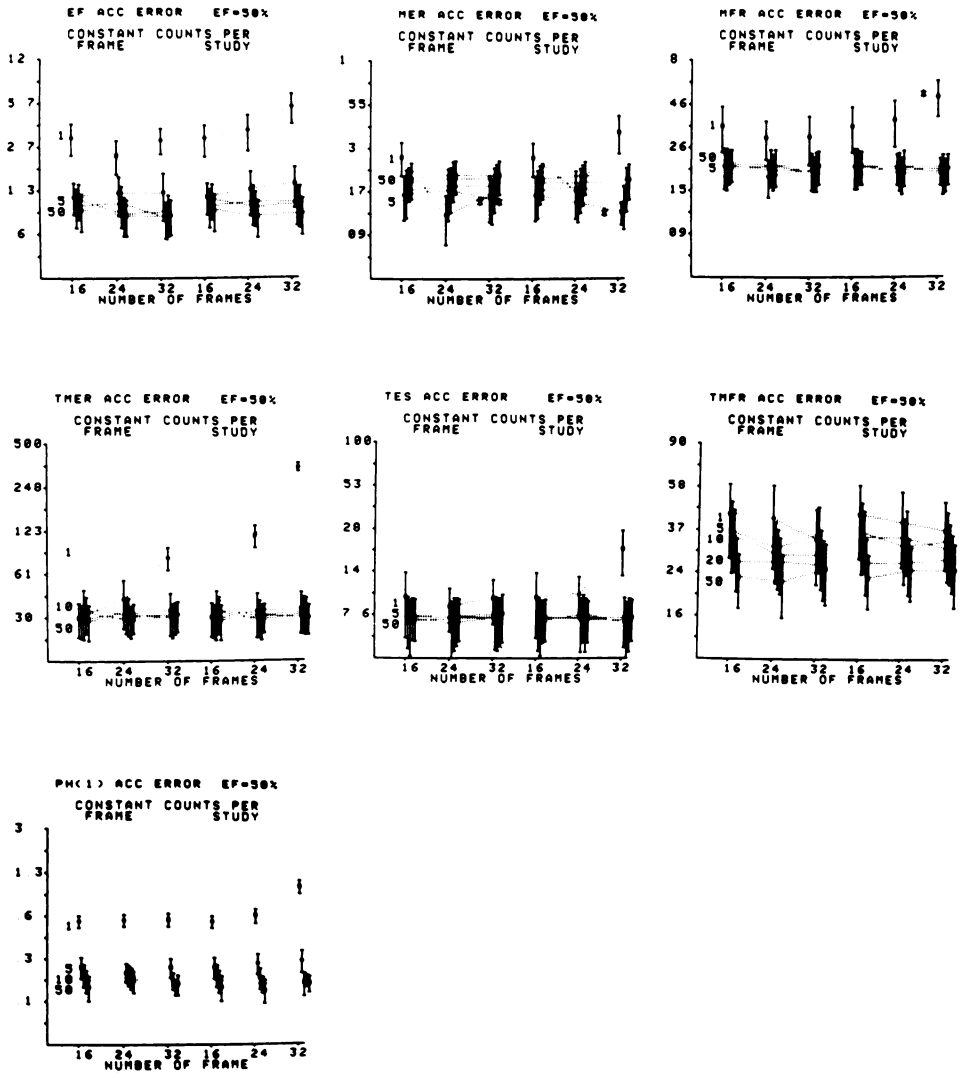

FIG. 3. Root-mean-square accuracy errors (± s.e.m.), plotted (with log ordinate) as function of framing rate, with pixels per segment (counts per frame) as parameter. Errors are calculated: ejection fraction (EF, %), maximum ejection rate (MER, end-diastolic volumes/sec), maximum filling rate (MFR, end-diastolic volumes/sec), time of maximum ejection rate (TMER, msec), time of end systole (TES, msec), time of maximum filling rate (TMFR, msec), and first-harmonic phase (PH_1) degrees. * = $p < 0.05$ for differences in values at 16 and 32 frames per cycle.

the framing rate constant. As the framing rate increases at constant counts per study (at the expense of counts per frame), precision error generally remains the same.

The behavior of the large precision error of the parameters calculated from segments one pixel in size tends to be unpredictable at different ejection fractions among the various parameters.

The accuracy error of the calculated parameters under the various conditions was measured by the RMS of the discrepancies between the mean parameter values for the noisy curves and the corresponding original noiseless curves.

As the ejection fraction increases, the absolute accuracy error for the segments of five or more pixels remains the same for EF, TMER, TES, and TMFR, decreases for PH_1, and increases for MER and MFR. The percent relative accuracy error of MER and MFR does remain the same, however, and decreases for EF. Accuracy error decreases for all parameters in a one-pixel segment. Figure 3 illustrates the data at an ejection fraction of 50%. As the counts per frame are increased by increasing the segment size (or count density), accuracy error decreases for TMFR. For the other parameters, accuracy error decreases only when the segment size is increased between one and five pixels, and remains the same for segments of five or more pixels. When the framing rate increases at constant counts per frame, accuracy remains the same for all parameters. As the framing rate increases at constant counts per study (at the expense of counts per frame) the accuracy error is unchanged except for a single-pixel segment, where the accuracy error tends to increase.

DISCUSSION

Precision and accuracy describe two different aspects of any measurement. Precision measures the variation of the measured parameter about its mean. In this study it is principally random counting error. Accuracy error, on the other hand, refers to the deviation of the measured parameter mean from its ideal value, and reflects systematic or built-in error.

Some results of this study are not surprising. An increase in total counts generally reduces the precision error. Clinically, this corresponds to selecting a larger segment of the ventricle for regional analysis, increasing the photon flux, or increasing imaging time. Parametric images using regions one pixel in size, while allowing for maximal spatial resolution, introduce unacceptable precision error, precluding their use for quantitative clinical analysis of gated images. Spatial smoothing, often performed before parameteric image construction, is equivalent to the sampling of larger segments, and results in smaller error.

The analysis of normal or hyperkinetic myocardial segments is more precise than the analysis of hypocontractile segments. This is supported by recent studies (*14*,*15*) and has implications for methods that measure the dispersion of temporal parameters, e.g., the first-harmonic phase, as an index of regional dysfunction (*3*). Therefore caution in interpretation is indicated, and a means of compensation for changing signal-to-noise ratio should be considered (*16*).

When total counts in the entire acquisition are limited—an event commonly encountered in exercise studies—an increased framing rate results in decreased counts per frame. Although it is commonly believed that temporal resolution is increased with higher framing rate, our results indicate that the precision error of the parameters remains unchanged. As a corollary, when the counts per frame are doubled, the error of all the parameters is the same as that produced by doubling of the framing rate.

For segments five pixels or more in size, the accuracy error appears to be independent of the counts per frame, segment size, and ejection fraction. At low counts per frame (one- to five-pixel segments), the accuracy error is large at low ejection fractions, and improves with increasing counts per frame and/or ejection fraction. Thus the system has a threshold, beyond which any further increase in signal-to-noise ratio does not affect the accuracy error. One exception to this is the first-harmonic phase, whose small accuracy error continues to decrease at higher ejection fraction.

The constancy of the accuracy error with increasing framing rate at constant counts per frame (except for one-pixel segments) is due to the filtering away of high-frequency information by the limited number of harmonics used.

The constancy of the accuracy error with increasing framing rate at constant total counts further supports the conclusion that little is gained by framing at a higher rate when the total counts are limited. This does not conflict with the results of Bacharach et al. (*17*), who found minimal framing requirements of 40 to 50 msec at rest, and 20 msec at exercise, for stable values of parameters derived from global left-ventricular time-activity curves. The present study examines sampling intervals of 50 msec or less at rest (16- to 32-frame study). During exercise the sampling interval decreases directly with the shorter cycle duration at the same framing rate.

The often deviant results for the one-pixel segment may be due to the dependence of all parameters except PH_1 on the peak or minimal values of the time-activity curve or its rate of change, leading to a unidirectional bias that is most evident in noisy curves. Bias in the Monte Carlo generator itself was excluded by extensive testing.

This study examines the effects of noise on regional parameters. The clinical choice of an appropriate segment size depends upon the specific application and its requirements of the analysis. Any decision involves a trade-off between spatial resolution and precision error. Figures 2 and 3 can be used as a guide for estimating the expected precision and accuracy errors under the specified conditions of pixel count density, region size, framing rate, and ejection fraction. For an average 50- to 200-pixel ventricle with 300 counts per pixel, or its equivalent, a segment size of five to 20 pixels may be used for regional analysis with generally acceptable precision and accuracy. The division of the ventricle into three to four segments appears to be adequate for the study of gross timing or contractile abnormalities (*6*,*9*). The best compromise for the detection of the effects of coronary artery disease may be four to eight segments. Although spatial smoothing limits the spatial resolution in parametric imaging to several pixels, quantitative information extracted from these images and from fine segmental subdivision of the ventricle should be interpreted with caution. This is also supported by the work of others (*14*,*18*–*20*).

Based on our previous studies, we chose to present data for three harmonics as the cutoff frequency. Three harmonics provide an optimal balance between precision and accuracy error for areas of five to 20 pixels in size (Figs. 2 and 3). Whereas an increase in the number of harmonics improves accuracy, it also causes an increase in precision error. A smaller number of harmonics has the opposite effect. Bacharach et al. (*21*) have recently shown in their system that two harmonics may be sufficient for systolic parameters, while three to five harmonics may be optimal for diastolic parameters. Although custom tailoring may ultimately be utilized for certain shapes of curves and individual variables, we present data for the best single compromise.

We used a square-shaped filter function, previously adopted by us and others (*9,21*), as opposed to a gradual roll-off filter. Our previous studies have shown that changes in the effects of "ringing" (Gibbs phenomenon) with a gradual roll-off filter are small compared with the effects of sampling noise and limitations of fit with few harmonics. For global, high-count time-activity curves, the Gibbs phenomenon will indeed be reduced by the use of higher-order harmonics and a filter less abruptly shaped.

Although we chose five curves commonly encountered clinically, clearly other variations exist. While there were differences in the magnitude of the parameter error among the five curves chosen, the behavior of the errors was quite uniform. The choice of parameter was divided between those measuring the amount and vigor of contraction (EF, MER) and relaxation (MFR) and their timing (TES, TMER, TMFR). First harmonic phase was examined because of its popularity for some applications. A more comprehensive review might include a larger choice of variables, a greater number of harmonic combinations, and additional curves.

In summary, this study is helpful in establishing the limits of confidence for measurements obtained from multiharmonic Fourier analysis of gated blood-pool studies. It should be useful in the selection of an optimal acquisition protocol, given the common clinical constraints of limited acquisition time, radionuclide dosage, and allowable error magnitude.

ACKNOWLEDGMENT

This work was supported in part by the Rippel Foundation and Bernard and Josephine Chaus through the Heart Research Foundation.

REFERENCES

1. ADAM WE, SIGEL H, GEFFERS H, et al: Analyse der regionalen wandbewegung des linken ventrikels bei koronarer herzkrankung durch ein nichtinvasives verfahren (radionuklid-kinematographie). *Z Kardiol* 66:545-555, 1977
2. ADAM WE, TARKOWSKA A, BITTER F, et al: Equilibrium (gated) radionuclide ventriculography. *Cardiovasc Radiol* 2:161-173, 1979
3. PAVEL D, BYROM E, SWIRYN S, et al: Normal and abnormal electrical activation of the heart: Imaging patterns obtained by phase analysis of equilibrium cardiac studies. In *Medical Radionuclide Imaging 1980*, vol II, Vienna, IAEA 1981, pp 253-261
4. BOTVINICK E, DUNN R, FRAIS M, et al: The phase image: Its relationship to patterns of contraction and conduction. *Circulation* 65:551-560, 1982
5. MACHAC J, MICELI K, HOROWITZ SF, et al: Quantification of regional ventricular function with vector Fourier analysis of gated images. In *IEEE 1982 Computers in Cardiology*. Ripley, K, ed. IEEE Computer Society Press, 1983, pp 303-306
6. MACHAC J, HOROWITZ SF, MICELI K, et al: Quantification of cardiac conduction abnormalities using segmental vector Fourier analysis of radionuclide gated blood pool scans. *J Am Col Cardiol* 2:1099-1106, 1983
7. WENDT RE, MURPHY PH, CLARK JW JR, et al: Interpretation of multigated Fourier functional Images. *J Nucl Med* 23:715-724, 1982
8. DECONINCK F, BOSSUYT A, LEPOUDRE R: Temporal contrast enhancement for the visual study of dynamic time patterns in scintigraphic image series. *J Nucl Med* 23:P67, 1982 (abstr)
9. MACHAC J, HOROWITZ SF, HALPERIN J, et al: Four chamber timing analysis in patients with programmable A-V sequential pacemakers using multiharmonic Fourier analysis of gated images. *J Nucl Med* 24:P92, 1983 (abstr)
10. HAMMERMEISTER KE, BROOKS RC, WERBASSE JR: The rate of change of left ventricular volume in man. I. Validation and peak systolic ejection rate in health and disease. *Circulation* 49:729-738, 1974
11. HAMMERMEISTER KE, WERBASSE JR: The rate of change of left ventricular volume in man. II. Diastolic events in health and disease. *Circulation* 49:739-747, 1974
12. MARSHALL RC, BERGER HJ, COSTIN JC, et al: Assessment of cardiac performance with quantitative radionuclide angiocardiography. Sequential left ventricular ejection fraction, normalized left ventricular ejection rate, and regional wall motion. *Circulation* 56:820-829, 1977
13. SOKAL RR, ROHLF FJ: *Biometry*. San Francisco and London, WH Freeman and Co. 1969, pp 320-333
14. HALAMA JR, HOLDEN JE: The effect of stochastic pixel noise on the distributions of magnitude and phase values in the Fourier Analysis of gated studies. *J Nucl Med* 24:P17, 1983 (abstr)
15. GREEN MV, BACHARACH SL, JONES-COLLINS BA, et al: A method for improving the specificity of phase analysis for regional defects in the presence of depressed global left ventricular function. *J Nucl Med* 24:P17, 1983 (abstr)
16. BACHARACH SL, GREEN MV, BONOW RO, et al: A method for objective evaluation of functional images. *J Nucl Med* 23:285-290, 1982
17. BACHARACH SL, GREEN MV, BORER JS, et al: Left ventricular peak ejection rate, filling rate, and ejection fraction frame rate requirements at rest and exercise: Concise communication. *J Nucl Med* 20:189-193, 1979
18. BACHARACH SL, GREEN MV, VITALE D, et al: Optimum number of harmonics for fitting cardiac volume curves. *J Nucl Med* 24:P17, 1983 (abstr)
19. MUKAI T, TAMAKI N, YONEKURA Y, et al: Optimum order harmonics of Fourier analysis in multigated blood-pool studies. *J Nucl Med* 24:P17, 1983 (abstr)
20. DOUGLAS MA, BAILEY JJ, VAN RIJK PP, et al: Analysis of regional function in radionuclide ventriculography: physiological signal, scintillation noise, and regional size. In *IEEE 1982 Computers in Cardiology*. Ripley, K, ed. IEEE Computer Society, 1983, pp 315-318
21. BACHARACH SL, GREEN MV, VITALE D, et al: Optimum fourier filtering of cardiac data: A minimum error method: Concise communication. *J Nucl Med* 24:1176-1184, 1983